Journal of Dental Research
2023, Vol. 102(1) 53–60

DOI: 10.1177/00220345221123253
journals.sagepub.com/home/jdr

Increased Handpiece Speeds without Air Coolant: Aerosols and Thermal Impact

J.J. Vernon[1*], P.E. Lancaster[2*], E.V.I. Black[1], D.A. Devine[1], L. Fletcher[3], D.J. Wood[1], and B.R. Nattress[2]

Abstract

This study assessed the impact of increased speed of high-speed contra-angle handpieces (HSCAHs) on the aerosolization of a severe acute respiratory syndrome coronavirus 2 (SARS-CoV-2) surrogate virus and any concomitant thermal impact on dental pulp. A bacteriophage phantom-head model was used for bioaerosol detection. Crown preparations were performed with an NSK Z95L Contra-Angle 1:5 (HSCAH-A) and a Bien Air Contra-Angle 1:5 Nova Micro Series (HSCAH-B) at speeds of 60,000, 100,000, and 200,000 revolutions per minute (rpm), with no air coolant. Bioaerosol dispersal was measured with Φ6-bacteriophage settle plates, air sampling, and particle counters. Heating of the internal walls of the pulp chambers during crown preparation was assessed with an infrared camera with HSCAH-A and HSCAH-B at 200,000 rpm (water flows ≈15 mL min^{-1} and ≈30 mL min^{-1}) and an air-turbine control (≈23.5 mL min^{-1}) and correlated with remaining tissue thickness measurements. Minimal bacteriophage was detected on settle or air samples with no notable differences observed between handpieces or speeds ($P > 0.05$). At all speeds, maximum settled aerosol and average air detection was 1.00 plaque-forming units (pfu) and 0.08 pfu/m^3, respectively. Irrespective of water flow rate or handpiece, both maximum temperature (41.5°C) and temperature difference (5.5°C) thresholds for pulpal health were exceeded more frequently with reduced tissue thickness. Moderate and strong negative correlations were observed based on Pearson's correlation coefficient, between remaining dentine thickness and either differential ($r = -0.588$) or maximum temperature ($r = -0.629$) measurements, respectively. Overall, HSCAH-B generated more thermal energy and exceeded more temperature thresholds compared to HSCAH-A. HSCAHs without air coolant operating at speeds of 200,000 rpm did not increase bioaerosolization in the dental surgery. Thermal risk is variable, dependent on handpiece design and remaining dentine thickness.

Keywords: SARS-CoV-2, COVID-19, bacteriophages, dental pulp, iatrogenic disease, thermography

Introduction

We recently demonstrated the efficacy of high-speed contra-angle handpieces (HSCAHs) for the reduction of potentially pathogenic, viral aerosols arising from the oral cavities of dental patients (Vernon et al. 2021). The novel use of a Φ6 bacteriophage marker as a proxy for severe acute respiratory syndrome coronavirus 2 (SARS-CoV-2) in the comparisons of aerosol mitigation strategies was received as a progressive step in the investigations of aerosol-generating procedures (AGPs) (Meurman 2021). Those investigations were essential amid a pandemic, to provide evidential support for the use of HSCAHs at low speeds (60,000 revolutions per minute [rpm]) as non-aerosol-generating tools to restart dental activities. However, the reduced cutting efficacy results in notably longer procedural times, potentially compounding transmission risk. Therefore, the desire to use these handpieces at greater speeds to improve cutting proficiency has inspired recent studies to investigate this issue (Allison et al. 2021). Using a fluorescein tracer and particle analysis, the authors demonstrated that with electric micromotors operated at 200,000 rpm and no airflow (water flow rate 61 mL min^{-1}), no detectable aerosol was measured beyond 1.5 m from the procedural origin. While these results are encouraging, the absence of a viral marker is a significant limitation in representing a more complete picture of transmission (Vernon et al. 2021).

Iatrogenic injury from dental treatment, such as cavity and crown preparation, may cause dehydration and/or inadvertently expose the pulp (Bergenholtz 1990; Brännström 1996), with up to 19% of vital teeth showing signs of periapical disease following crown preparation (Saunders and Saunders 1998). Temperature increases of 5.5°C and 11.1°C in pulp of rhesus monkeys led to irreversible pulpitis of 15% and 60% of teeth, respectively (Zach and Cohen 1965; Zach 1972). The reported threshold for initiating pulp inflammation was identified as 41.5°C, with 44.6°C resulting in pain.

[1]Division of Oral Biology, School of Dentistry, University of Leeds, Leeds, UK
[2]Division of Restorative Dentistry, School of Dentistry, University of Leeds, Leeds, UK
[3]School of Civil Engineering, University of Leeds, Leeds, UK
*Authors contributing equally to this article.

A supplemental appendix to this article is available online.

Corresponding Author:
D.J. Wood, Division of Oral Biology, School of Dentistry, Worsley Building, Clarendon Way, University of Leeds, LS2 9JT, UK.
Email: d.j.wood@leeds.ac.uk

The blood supply of the pulp is thought to act as a heat sink in vivo, removing excessive heat or supplying heat when cooled. Furthermore, enamel and dentine are thermally protective, insulating the vital pulp tissue, although demineralized carious enamel and dentine are reported to be less protective than sound tissue (Lancaster et al. 2017). The thickness of enamel and dentine in human teeth ranges widely with daily, physiological deposits of secondary dentine (≈0.8 µm) (Pashley 1996) and tertiary dentine deposited locally in response to stimuli (e.g., abrasion, attrition, erosion, and caries). Tissue thickness is least in the middle-cervical region, an area often prepared for extracoronal restorations (Peters et al. 1994; Ruddle 2002).

With the recent reported risk of dental AGPs following coronavirus disease 2019 (COVID-19), attention has focused on finding alternative handpieces to air turbines that do not generate the same level of aerosol risk to patients and dental care professionals but still satisfactorily and safely prepare teeth. Modern HSCAHs use air and water to cool, lubricate, and clean the cutting bur, thus reducing energy transfer to the tooth. One recent study indicated that the use of an HSCAH with only water coolant can result in acceptable temperature increases (Lempel and Szalma 2021). This was reported as highly dependent on the water flow rate when the remaining dentine thickness was 1 mm. When used with a 30 mL min^{-1} coolant flow, the temperature increase recorded by a thermocouple was within the acceptable threshold for limiting pulpal damage, of 5.5°C. However, when the flow was reduced to 15 mL min^{-1}, the temperature increase reached an unacceptable level of 6.9°C. Özturk and colleagues (2004) reported a flow rate of 40 mL min^{-1} and avoided exceeding the critical temperature change of 5.5°C. This was also recorded with a thermocouple, following a single cutting action into the tooth, leaving a mean dentine thickness of 1.02 mm (Öztürk et al. 2004). A limitation of this and other such temperature measurements recorded through conduction with contact devices (e.g., thermocouples, thermometers, and thermistors) is that they provide a small point of contact and may not record the area of greatest temperature change within the pulp chamber. Contactless devices (e.g., thermal cameras) can capture radiation from a larger, user-defined area. We propose that thermal imaging using an infrared camera will overcome some of the limitations of conduction-based methods. Clearly, combining viral transmission and thermal impact data of the handpieces used in the absence of air coolant is necessary to allow recommendations for future clinical practice. For this study, we hypothesize that 2 representative HSCAHs run without air, at 200,000 rpm, will demonstrate no risk of bioaerosolization or excessive heating of the pulp chamber.

Accordingly, in this study, we used the bacteriophage biomarker model to assess the relationship between speed increases and viral dispersal in the dental setting. Furthermore, we assessed 2 common examples of micromotor HSCAHs at 200,000 rpm with 2 water flow rates (15 and 30 mL min^{-1}) and investigated the thermal impact on dental pulp using thermal imaging in an in vitro tooth model.

Methods

Viral Transmission Study

Microbiological strains and culture conditions. The bacteriophage Φ6 (DSM 21518) and the host organism *Pseudomonas syringae* (DSM 21482; German Collection of Microorganisms and Cell Cultures, Leibniz Institute) were cultured and propagated as previously reported (Vernon et al. 2021).

Experimental setup. Investigations were performed in a clinical surgery at the Leeds Dental Institute. As previously (Vernon et al. 2021), a dental simulation unit with an artificial salivary flow (1.5 mL min^{-1}; see Appendix) containing ~10^8 plaque-forming units (pfu) mL^{-1} was used to represent the upper concentrations of SARS-CoV-2 in human saliva as a worst-case scenario.

Experimental procedures. Full crown preparations were performed on the upper-left lateral incisor using 2 different HSCAHs. An NSK Z95L Contra-Angle 1:5 (NSK United Kingdom Ltd.; HSCAH-A, water flow rate 60 mL min^{-1}) and a Bien Air Contra-Angle 1:5 Nova Micro Series (Bien Air (UK) Ltd.; HSCAH-B, flow rate 32 mL min^{-1}) were used at 3 different speeds (60,000, 100,000, and 200,000 rpm), in the absence of air coolant (often referred to as "chip air"). Procedures comprised 4 min of cutting followed by 1 min of rest, repeated 4 times with high-volume aspiration. A 10-min, preprocedural settle period and a 20-min postprocedural fallow period were used. Each procedure was repeated in triplicate (Fig. 1).

Data collection. Aerosolization was determined as previously (Vernon et al. 2021), through Φ6 bacteriophage settle plates lawned with *P. syringae*, MicroBio MB2 (Cantium Scientific) air sampling, and Kanomax 3889 GEOα particle counters (Kanomax). Further details are outlined in the Appendix. Multiple comparisons were performed in IBM SPSS Statistics V.26.0.0.0 using a Mann–Whitney *U* test and Bonferroni correction. *P* values <0.05 were deemed significant.

High-speed photography. High-speed photographs of the HSCAH tips activated at 60,000, 100,000, and 200,000 rpm were taken with a Photron FASTCAM Mini AX200 with a 24- to 70-mm zoom lens, F28, 1/20,000s, 6,400 frames per second.

Thermal Impact Study

Human teeth samples. Nine dry, sound human molar teeth (DREC ref:160821/PL/330) were disinfected with Distel (Tristel Solutions Ltd.) and stored in phosphate-buffered saline. Photographs and radiographs (60 kV, 0.125 s) were taken pre- and postpreparation.

Teeth were halved using an Accustom-5 (Struers), and remaining pulp tissue was removed. All samples were refrigerated until needed, with 24 h allowed prior to crown preparation

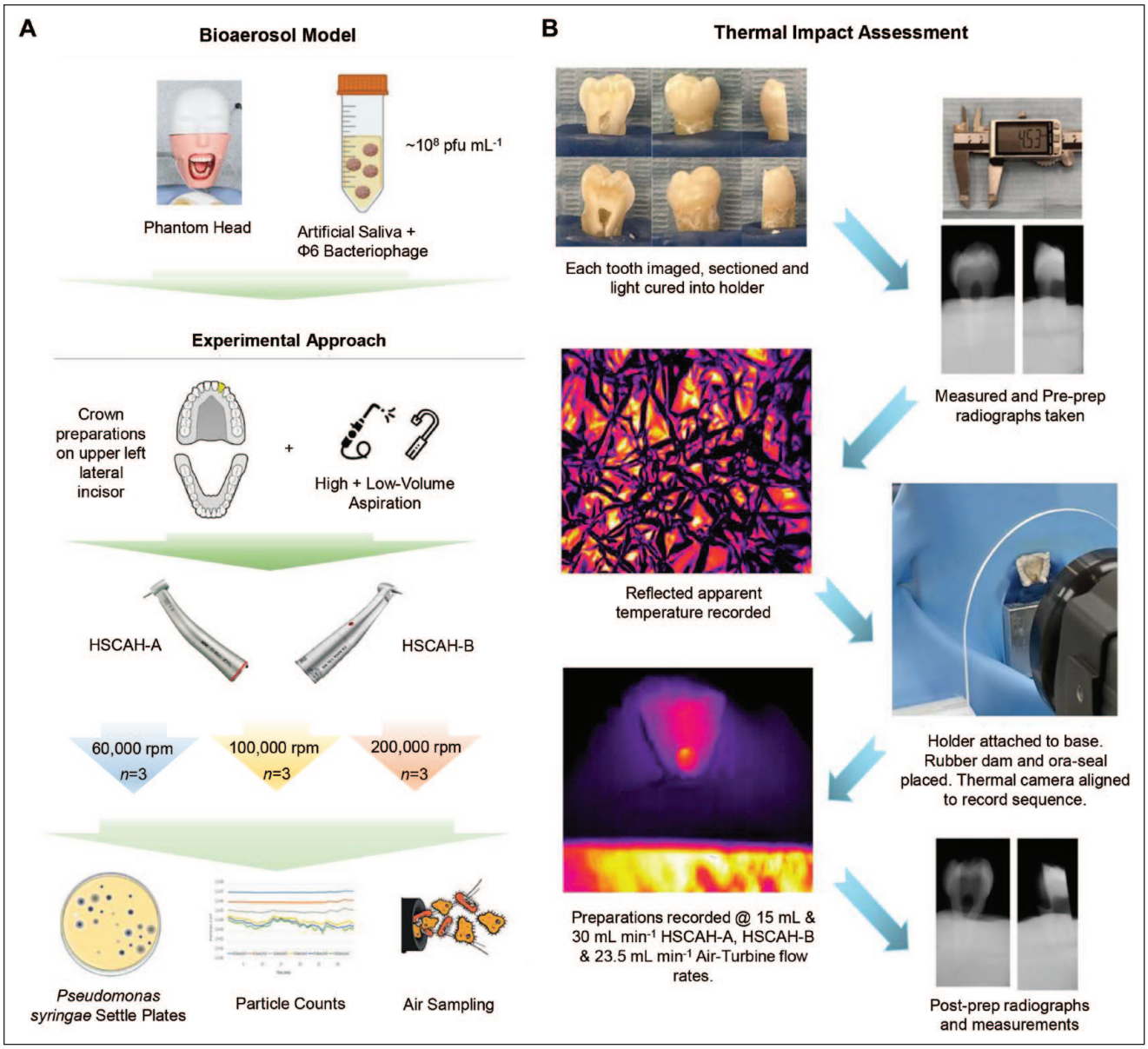

Figure 1. Experimental design flow diagrams. (**A**) Experimental setup including procedural position, handpiece, and mitigation variables tested, outlined with data collection methods. (**B**) Experimental setup for tooth preparation and thermal data collection. HSCAH-A, highspeed contra-angle handpiece A; HSCAH-B, highspeed contra-angle handpiece B; pfu, plaque-forming units.

for thermal stabilization to room temperature. Sample dimensions were recorded with a digital caliper customized with a 0.7-mm orthodontic wire.

Experimental setup. The sectioned teeth were embedded using light-cured resin (Bracon Dental Laboratories) in a bespoke aluminum holder, screwed to a stable metal base. A medium-gauge dental rubber dam sheet (152 × 152 mm; Unodent) was placed around each sample and attached to a rubber dam frame set in silicone on the metal base. A waterproof seal was achieved using Oraseal caulking (Optident Ltd.). An additional Perspex shield with a small viewing window was placed between the thermal camera and the preparation.

A new diamond bur (Dentsply 556 Fine Shoulder; Dentsply Sirona) was used for each preparation. Partial crown preparations were performed (n = 18) by the same experienced operator on each sample using HSCAH-A (n = 7) and HSCAH-B (n = 9) at 200,000 rpm, in the absence of "chip air." Two control samples were prepared using a KaVo EXPERTtorque LUX E680L air turbine at 23.5 mL min^{-1} (KaVo Dental Ltd.). Preparations were carried out at flow rates of 15 mL min^{-1} (n = 4) and 30 mL min^{-1} (n = 12) using both HSCAHs. Water flow rate determination is outlined in the Appendix.

Temperature measurement and data collection. A FLIR SC325 thermal camera (FLIR Systems), with a ×4 lens at a focal

Table. Phage Detection Data Clustered into Splatter and Aerosol Groups.

	Pfu, Mean ± SD						
	HSCAH-A			HSCAH-B			Previous Data
Characteristic	60,000 rpm (*n* = 3)	100,000 rpm (*n* = 3)	200,000 rpm (*n* = 3)	60,000 rpm (*n* = 3)	100,000 rpm (*n* = 3)	200,000 rpm (*n* = 3)	60,000 rpm (*n* = 3)
Splatter zone	8.33 ± 3.53	64.67 ± 37.98	60.33 ± 14.68	45.00 ± 4.04	56.67 ± 4.48	49.33 ± 4.63	64.33 ± 61.84
Settled aerosol	0.00 ± 0.00	1.00 ± 1.00	1.00 ± 1.00	0.00 ± 0.00	0.00 ± 0.00	0.00 ± 0.00	0.00 ± 0.00
Average air (pfu/m^3)	0.08 ± 0.08	0.08 ± 0.08	0.08 ± 0.04	0.00 ± 0.00	0.00 ± 0.00	0.04 ± 0.04	0.10 ± 0.04
Fallow settle	0.00 ± 0.00	0.00 ± 0.00	0.67 ± 0.67	0.00 ± 0.00	0.00 ± 0.00	0.00 ± 0.00	0.00 ± 0.00
Average fallow air (pfu/m^3)	0.00 ± 0.00	0.00 ± 0.00	0.00 ± 0.00	0.00 ± 0.00	0.00 ± 0.00	0.00 ± 0.00	0.00 ± 0.00

Previous data refer to HSCAH-A used at 60,000 rpm as found in Vernon et al. (2021).
HSCAH-A, highspeed contra-angle handpiece A; HSCAH-B, highspeed contra-angle handpiece B; pfu, plaque-forming units.

distance of ≈8 cm, spatial resolution of 100 µm, and thermal sensitivity of <0.05°C captured 30 frames per second. Reflected apparent temperature was assessed for each recording session, and an emissivity of 0.95 was used for the internal dentine of the pulp wall (Lancaster 2018). The region of interest (the internal wall of the pulp chamber) was drawn freehand within the FLIR ResearchIR Max software (FLIR Systems) to record the average temperature of this area during crown preparation. The maximum temperature (°C) of the region of interest was ascertained for each preparation. The baseline starting temperature was subtracted from the maximum recorded temperature to give the change in temperature (Δ°C) during preparation. Thermal data were collected every second by the TC08 data logger software (Pico Technology) for room temperature. In addition, the duration of each preparation was recorded. Descriptive statistics were evaluated with IBM SPSS Statistics V.26.0.0.0.

Results

Viral Transmission Study

Bacteriophage marker detection. Across all experimental procedures, bacteriophage detection was low (Table), except for in the splatter zone (range 8.33–64.67 pfu). No settled aerosol was detected with HSCAH-B at all speeds, with only 1.00 (±1.00) pfu detected at 100,000 and 200,000 rpm with HSCAH-A ($P > 0.05$; Fig. 2). Average air concentrations were very low, with 0.08 (±0.08) pfu/m^3 recovered at all speeds with HSCAH-A and only 0.04 (±0.04) pfu/m^3 detected at 200,000 rpm with HSCAH-B ($P > 0.05$). No phage was detected with HSCAH-B at 60,000 or 100,000 rpm. Only 1 procedure recorded phage on the fallow period settle plates, representing 1 procedural replicate using HSCAH-A at 200,000 rpm. No bacteriophage plaques were identified from the fallow period air samples for either handpiece.

Particle data. The particle data presented similar trends between the HSCAHs, with no clear correlation between speed increases and particle production (Appendix Table 2/Appendix Fig. 2). Counts of the smallest particles (0.3 µm and 0.5 µm) ranged between 9.56×10^2 to 1.28×10^5 and 7.20×10^3 to 2.53×10^5 per m^3 for HSCAH-A and HSCAH-B, respectively.

High-speed photography. The increased flow rate of HSCAH-A over HSCAH-B can clearly be seen in the high-speed images (Fig. 3), with far more droplet formation and spray visible. Escalating levels of radial atomization were observed with both handpieces at speeds >60,000 rpm. This was more apparent with HSCAH-A due to its higher water flow rate.

Thermal Impact Study

Multiple variables may influence the thermal impact of tooth preparation, and these are ordered from the perspective of water flow rate and handpiece in Appendix Figure 7, which demonstrated no relationship of preparation time or room (20.5°C–22.7°C) or water coolant (19.9°C–22.8°C) temperature in exceeding either thermal threshold.

Removal of these variables and ordering from the perspective of the remaining tissue thickness demonstrated a clear relationship with the thermal thresholds (Fig. 4). Pearson's correlation coefficients indicated moderate and strong correlations for both differential ($r = -0.588$) and maximum temperature ($r = -0.629$) metrics, respectively. In addition, pulp safety thresholds were exceeded more frequently with lower remaining tissue thicknesses; furthermore, this relationship was more apparent with HSCAH-B compared with HSCAH-A (Fig. 4).

Comparisons indicated potential differences in maximum temperatures between HSCAH-A (mean ± SD: 33.61°C ± 4.76°C) and HSCAH-B (mean ± SD: 41.56°C ± 12.94°C), with HSCAH-B exceeding the 95% confidence interval of 29.21°C to 38.01°C. Similar differences were observed with the change in temperature, HSCAH-A (mean ± SD: 7.20°C ± 3.98°C) and HSCAH-B (mean ± SD: 14.49°C ± 12.34°C), again with HSCAH-B exceeding the 95% confidence interval of 3.51°C to 10.88°C. Based on the thermal transfer data, the study hypothesis was rejected.

An example video demonstrating the thermal exchange captured with the thermal camera during crown preparation with HSCAH-B at a 30-mL min^{-1} flow rate is shown in Appendix Video 1.

Figure 2. Heatmap representation of bacteriophage dispersal in the dental surgery, delineated by handpiece and cutting speed. Circles represent settle plate sampling points, gray (multiple time points) and white (single time point). Data from Vernon et al. (2021) for an air turbine are displayed as a comparator. Heatmaps were created using image overlay function of http://www.heatmapper.ca. pfu, plaque forming units.

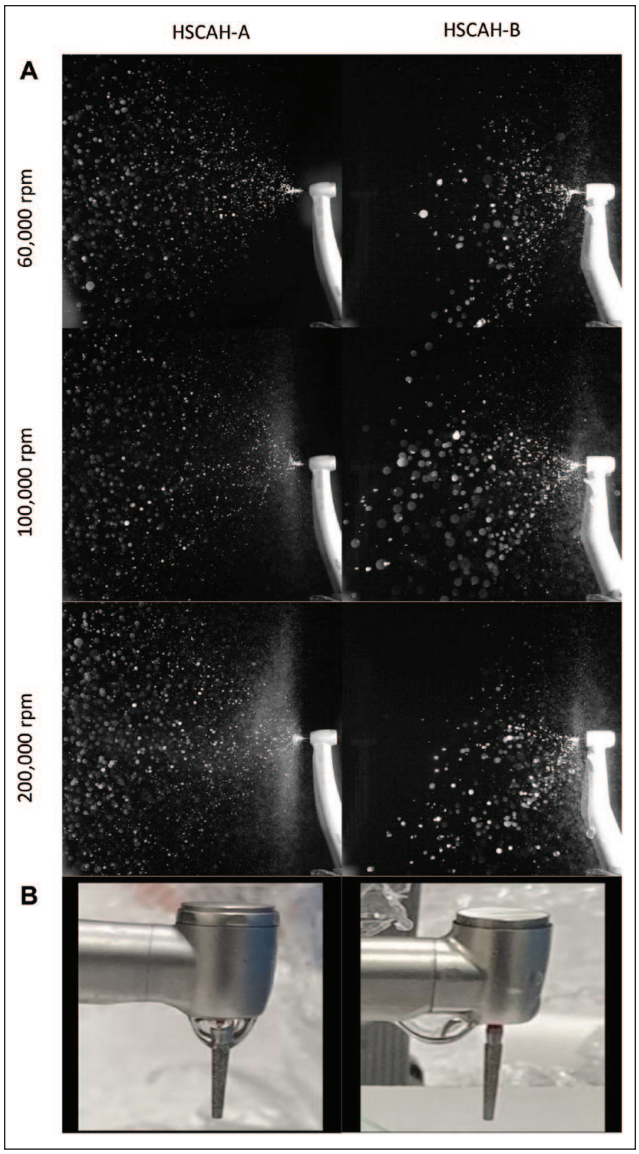

Figure 3. Contra-angle high-speed handpiece tip images taken during and postactivation. (**A**) HSCAH-A at 15 mL min^{-1} (left) and HSCAH-B at 30 mL min^{-1} (right) handpiece tips at 60,000, 100,000, and 200,000 rpm demonstrating the water coolant droplet size and degree of atomization. Images taken with a Photron FASTCAM Mini AX200 with a 24- to 70-mm zoom lens, F28, 1/20,000 s, 6,400 frames per second and processed with Photron FASTCAM Viewer 4, v.4.0.4.1. (**B**) Water droplet position after use of HSCAH-A (left) and HSCAH-B (right). Irrespective of the flow rate, water settled around the bur insertion in HSCAH-A, whereas the water settled behind the bur for HSCAH-B. HSCAH-A, highspeed contra-angle handpiece A; HSCAH-B, highspeed contra-angle handpiece B.

Discussion

Here we have built upon our previous model investigations using Φ6 bacteriophage as a marker for SARS-CoV-2 to investigate the crucial, next question of whether there is an increased risk of bioaerosol dispersal or thermal damage at greater cutting speeds. While our previous study validated many of the decisions made regarding AGPs and HSCAHs at low speeds (Vernon et al. 2021), this work aimed to provide data to support improvements to the efficiency of procedures by assessing the use of HSCAHs at faster speeds. It thus aims to support decisions around increasing access and dental activity for patients, balanced with protecting the dental workforce and patients as a vital step in learning to live with COVID-19.

Two typical examples of HSCAHs were tested due to their substantial differences in flow rates, ensuring greater translatability of the findings. Importantly, bacteriophage detection during experimental procedures with both handpieces run at

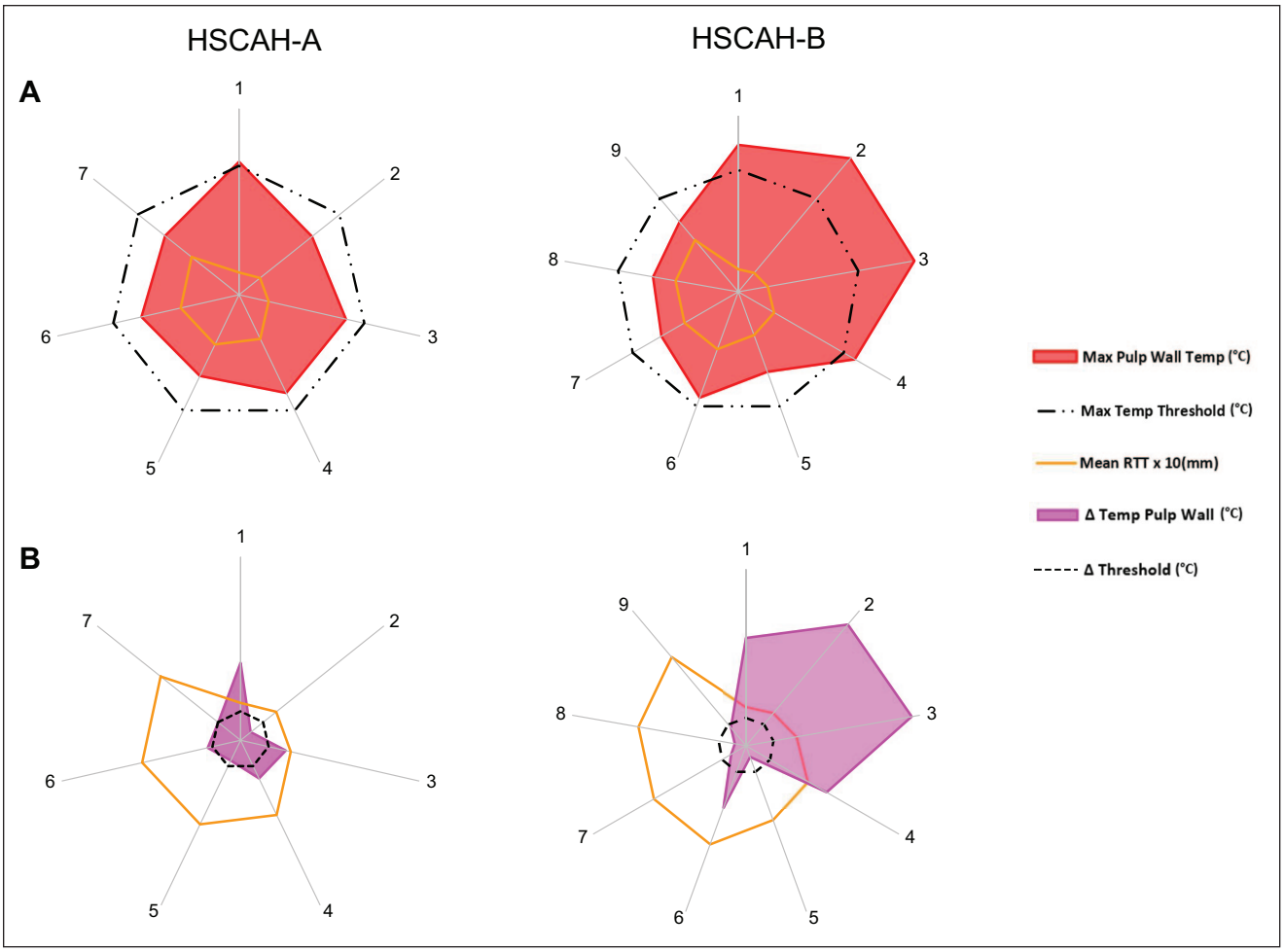

Figure 4. Radar charts ordered for increasing remaining tooth tissue (mm), outlining the relationships between handpieces, remaining tooth tissue (RTT), and pulp temperatures (HSCAH-A, left; HSCAH-B, right). (**A**) Maximum pulp wall temperature. HSCAH-A: 0.71 mm was the thinnest remaining tissue, prepared at 30 mL min^{-1}, and was the only sample to exceed this threshold at 42.84°C. All other preparations remained below this threshold with remaining tissue ranging from 0.87 to 1.78 mm at 30 mL min^{-1} and 1.93 to 1.95 mm at 15 mL min^{-1}. HSCAH-B: 0.78 mm was the thinnest remaining tissue and exceeded this threshold at 50.05°C, as did 3 further samples at 0.85 mm (59.36°C), 1.02 mm (60.91°C), and 1.42 mm (45.81°C), all prepared at 30 mL min^{-1}. All other preparations remained below this threshold with remaining tissue ranging from 1.57 to 2.3 mm with flow rates of 30 mL min^{-1} and 15 mL min^{-1}. (**B**) Difference in pulp wall temperature. HSCAH-A: 14.76°C was the greatest difference in temperature for 0.71 mm, at 30 mL min^{-1}, exceeding this threshold. Samples at 0.99 mm (8.87°C) and 1.59 mm (8.11°C) with flow rate of 30 mL min^{-1} and 1.93 mm (6.41°C) with flow rate of 15 mL min^{-1} also exceeded this threshold. Samples at 0.87 mm and 1.78 mm with flow rate of 30 mL min^{-1} and 1.95 mm with flow rate of 15 mL min^{-1} did not exceed this threshold. HSCAH-B: 33.31°C was the greatest difference in temperature for 1.02 mm, at 30 mL min^{-1}, exceeding this threshold. Samples at 0.78 mm (21.37°C), 0.85 mm (31.36°C), and 1.42 mm (18.43°C) at 30 mL min^{-1}, as well as 2.08 mm (13.14°C) at 15 mL min^{-1}, also exceeded this threshold. Samples at 1.57 mm, 2.11 mm, and 2.17 mm at 30 mL min^{-1} and 2.30 mm at 15 mL min^{-1} did not exceed this threshold. To summarize, 1 HSCAH-A and 4 HSCAH-B preparations exceeded the maximum temperature threshold all at 30 mL min^{-1} and 4 HSCAH-A and 5 HSCAH-B preparations exceeded the difference in temperature threshold at both 30 mL $min^{-1}$and 15 mL min^{-1}. HSCAH-B exceeded the thresholds with higher temperatures than HSCAH-A. HSCAH-A, highspeed contra-angle handpiece A; HSCAH-B, highspeed contra-angle handpiece B.

60,000 rpm was comparable to previous findings (Vernon et al. 2021). Speed increases in either handpiece did not generate any significant increases in bacteriophage detection on settle, air, or fallow samples (Table). These findings indicated the use of HSCAHs at greater speeds does not markedly contribute to the generation of viral aerosols, in the absence of chip air, building on the fluorescein tracer data reported for nonviral aerosols (Allison et al. 2021).

One fallow settle plate, for 1 experimental procedure using HSCAH-A at 200,000 rpm, exhibited 2 bacteriophage plaques. This was an outlying finding, with no detection across all other experimental procedures, suggesting minimal aerosol persists postprocedure with these parameters. Furthermore, no biomarker was recorded in the air during the fallow periods with either handpiece up to 200,000 rpm, increasing confidence in the absence of lingering bioaerosols. Moreover, particle levels for all size ranges and HSCAH speeds were comparable with those during our previous investigations (Vernon et al. 2021) while still demonstrating 2-log reductions versus the air turbine from the same study (Appendix Table 2).

With no evidence of increased viral aerosolization at higher cutting speeds, the potential for thermal damage in the absence of air cooling was essential to determine. This study has investigated the thermal impact from preparing a crown rather than a cavity as in many earlier studies. A new bur of the same design and manufacture was used on every preparation to negate for differences in burs, which have previously been shown to influence energy transfer (Segal et al. 2016). To maintain consistency across all procedures, preparations were performed by a single, experienced operator carrying out their normal clinical practice. Therefore, lateral drill pressures would reflect the variation of forces generated, and subsequent thermal impact, during a tooth preparation in the clinic. There was no statistical difference in the preparation times between the 2 handpieces, evidencing consistency of procedure.

The HSCAHs have been recommended to have a water flow rate of at least 50 mL min^{-1} (BS EN ISO 14457:2017) and up to 60 mL min^{-1} from some manufacturers (Bien Air (UK) Ltd.), which is quite challenging to manage clinically. Despite the use of aspiration, patients may find this volume of water difficult to tolerate, requiring pauses in the procedure, along with localized wetting from water droplets. In addition, the high flow rates often reduce visibility for the clinician and a requirement for additional water bottle refills. Both factors can lead to increases in appointment times. Therefore, a minimal flow rate is desirable. At a 15-mL min^{-1} water flow rate, concern has been expressed that a change of 5.5°C (the threshold to protect the pulp) can be exceeded with 1 mm remaining dentine thickness. Therefore, 30 mL min^{-1} was advised when using 200,000 rpm (Lempel and Szalma 2021). In that study, temperature was measured via a thermocouple, which also risks the peak temperature being missed compared to recording an area of interest as seen with the thermograph in this study.

The result of this study indicated the most important factors affecting thermal transfer to the pulp chamber were the handpiece design and the remaining tissue thickness. The remaining dentine during tooth preparation has a clinically significant role in protecting the pulp from temperature increases (Aguiar et al. 2005; Lipski et al. 2020). Above 1.42 mm remaining tissue, no maximum temperature was exceeded by HSCAH-A, HSCAH-B, or the air turbine when respective water flow rates of 15 mL min^{-1}, 30 mL min^{-1}, and 23.5 mL min^{-1} were used. It was interesting to note that in the preparations with greater remaining thickness, the temperature changes, even with lower flow rates, were less. The maximum temperature thresholds were exceeded with tissue thicknesses of 0.71 mm (HSCAH-A) and up to 1.02 mm (HSCAH-B). The difference in temperature thresholds was exceeded at remaining dentine thicknesses as high as 1.93 mm (HSCAH-A) and 2.08 mm (HSCAH-B). The air turbine controls were safely below both thresholds, with remaining tissue thickness as low as 1.17 mm.

The overall trend seen is that HSCAH-B exceeded more temperature threshold values on more occasions than HSCAH-A. Interestingly, HSCAH-A was designed to allow the air coolant to be turned off at the handpiece. The use of HSCAHs without air coolant arose as a response to reduce viral aerosol generation. During this study, it was apparent that the alignment of water jets to the bur in HSCAH-B was more variable that in HSCAH-A, and at the end of the procedure, the residual water drops settled behind the bur shank rather than on the bur (Fig. 3). This may have reduced the overall cooling effects on the bur and is an important consideration when using HSCAHs without air coolant.

One limitation of our model is the absence of simulated blood flow. However, flow rates for pulp are highly variable in the literature, ranging from 0.0042 mL min^{-1} (Park et al. 2010) to 60 mL min^{-1} (Aksoy et al. 2021). Since there is no consensus in this area, coupled with intertooth/patient variation, any blood flow rate selected would have been arbitrary. Addition of this parameter, while potentially useful, could either over- or underestimate temperatures. Here, we opted for the cautious approach to thermal modeling, representing a worst-case scenario, as we applied with the viral aerosolization work.

As previously reported (Vernon et al. 2021), where available, HSCAHs should be used to minimize potential aerosolization of SARS-CoV-2. This study goes further to suggest that using HSCAHs up to 200,000 rpm does not significantly increase viral aerosolization. These data contribute to the body of research informing updates to the clinical guidelines indicating safe use of HSCAHs at increased speeds, in the absence of air coolant. Where financial restrictions do not permit this switch, the recommendation to use a rubber dam is endorsed, supporting the current guidance (Gherlone et al. 2021).

Conclusion

For crown preparations, neither HSCAH used at 200,000 rpm generated notable bioaerosol. When considering the thermal impact at each of the water flow rates used, neither HSCAH, used at 200,000 rpm, exceeded the critical temperature change required to cause pulpal damage, provided the residual thickness of dentine was above 1.59 mm with a 30-mL min^{-1} water flow rate. Where concern over remaining dentine thickness exists, as seen in younger patients with larger pulp chambers, a flow rate of 30 mL min^{-1} with reduced rpm would be recommended.

Author Contributions

J.J. Vernon, P.E. Lancaster, D.J. Wood, B.R. Nattress, contributed to conception and design, data acquisition, analysis, and interpretation, drafted and critically revised the manuscript; E.V.I. Black, contributed to data acquisition, critically revised the manuscript; D.A. Devine, contributed to data conception and design, critically revised the manuscript; L. Fletcher, contributed to data design, critically revised the manuscript. All authors gave final approval and agree to be accountable for all aspects of the work.

Acknowledgments

The authors thank the Leeds Teaching Hospitals Trust for supplying clinical surgery space for the research and Mick Devlin for his technical skills.

Declaration of Conflicting Interests

The authors declared no potential conflicts of interest with respect to the research, authorship, and/or publication of this article.

Funding

The authors disclosed receipt of the following financial support for the research, authorship, and/or publication of this article: The funding for this research was in part funded by NSK United Kingdom Ltd. and Bien Air (UK) Ltd.

ORCID iDs

J.J. Vernon https://orcid.org/0000-0002-0072-9294
E. V.I. Black https://orcid.org/0000-0003-1600-1094
D.A. Devine https://orcid.org/0000-0002-8037-9254
D.J. Wood https://orcid.org/0000-0001-8269-9123

References

Aguiar FHB, Barros GKP, Santos AJS, Ambrosano GMB, Lovadino JR. 2005. Effect of polymerization modes and resin composite on the temperature rise of human dentin of different thicknesses: an in-vitro study. Oper Dent. 30(5):602–607.

Aksoy M, Şen S, Kaptan A, Büyükkok Ç, Tulga-Öz F. 2021. Does the heat generated by fluorescence-aided caries excavation system effect the pulp temperature of primary teeth irreversibly? An in-vitro evaluation of the temperature changes in the pulp chamber. J Clin Exp Dent. 13(11):e1096–e1103.

Allison JR, Edwards DC, Bowes C, Pickering K, Dowson C, Stone SJ, Lumb J, Durham J, Jakubovics N, Holliday R. 2021. The effect of high-speed dental handpiece coolant delivery and design on aerosol and droplet production. J Dent. 112:103746.

Bergenholtz G. 1990. Pathogenic mechanisms in pulpal disease. J Endodont. 16(2):98–101.

Brännström M. 1996. Reducing the risk of sensitivity and pulpal complications after the placement of crowns and fixed partial dentures. Quintessence Int. 27(10):673–678.

BS EN ISO 14457:2017. 2017. Dentistry—handpieces and motors.

Gherlone E, Polizzi E, Tetè G, Capparè P. 2021. Dentistry and Covid-19 pandemic: operative indications post-lockdown. New Microbiol. 44(1):1–11.

Lancaster P, Brettle D, Carmichael F, Clerehugh V. 2017. In-vitro thermal maps to characterize human dental enamel and dentin. Front Physiol. 8:461.

Lancaster PE. 2018. The feasibility of using infra-red radiation in determining tooth-vitality. PhD thesis. University of Leeds [accessed 2022 Aug 16]. https://etheses.whiterose.ac.uk/22141/.

Lempel E, Szalma J. 2021. Effect of spray air settings of speed-increasing contra-angle handpieces on intrapulpal temperatures, drilling times, and coolant spray pattern. Clin Oral Invest. 26(1):523–533.

Lipski M, Woźniak K, Szyszka-Sommerfeld L, Borawski M, Droździk A, Nowicka A. 2020. In vitro infrared thermographic assessment of temperature change in the pulp chamber during provisionalization: effect of remaining dentin thickness. J Healthc Eng. 2020:8838329.

Meurman JH. 2021. Do dental aerosols matter? J Dent Res. 100(13):1423–1424.

Öztürk B, Üşümez A, Öztürk AN, Ozer F. 2004. In vitro assessment of temperature change in the pulp chamber during cavity preparation. J Prosthet Dent. 91(5):436–440.

Park SH, Roulet JF, Heintze SD. 2010. Parameters influencing increase in pulp chamber temperature with light-curing devices: curing lights and pulpal flow rates. Oper Dent. 35(3):353–361.

Pashley DH. 1996. Dynamics of the pulpo-dentin complex. Crit Rev Oral Biol Med. 7(2):104–133.

Peters DD, Baumgartner JC, Lorton L. 1994. Adult pulpal diagnosis: I. Evaluation of the positive and negative responses to cold and electrical pulp tests. J Endodont. 20(10):506–511.

Ruddle CJ. 2002. Endodontic diagnosis. Dent Today. 21(10):90–101.

Saunders EM, Saunders WP. 1998. Peri-radicular status of crowned teeth in an adult Scottish subpopulation. J Dent Res. 77(spec iss B):672. Abstract #325.

Segal P, Sap D, Ben-Amar A, Levartovsky S, Matalon S. 2016. A comparison of temperature increases produced by "premium" and "standard" diamond burs: an in-vitro study. Quintessence Int. 47(2):161–166.

Vernon JJ, Black EVI, Dennis T, Devine DA, Fletcher L, Wood DJ, Nattress BR. 2021. Dental mitigation strategies to reduce aerosolization of SARS-CoV-2. J Dent Res. 100(13):1461–1467.

Zach L. 1972. Pulp lability and repair; effect of restorative procedures. Oral Surg Oral Med Oral Pathol. 33(1):111–121.

Zach L, Cohen G. 1965. Pulp response to externally applied heat. Oral Surg Oral Med Oral Pathol. 19(4):515–530.